UPPSALA
UNIVERSITET

UPTEC F 20010
Examensarbete 30 hp
Maj 2020

Measuring water current speed and direction of a long term underwater sensor (LoTUS) using tilt and roll compensation.

Author: Marcus Lindkvist
Supervisor: Jakob Kuttenkeuler
Subject reviewer: Uwe Zimmermann

UPPSALA
UNIVERSITET

Teknisk- naturvetenskaplig fakultet
UTH-enheten

Besöksadress:
Ångströmlaboratoriet
Lägerhyddsvägen 1
Hus 4, Plan 0

Postadress:
Box 536
751 21 Uppsala

Telefon:
018 – 471 30 03

Telefax:
018 – 471 30 00

Hemsida:
http://www.teknat.uu.se/student

Abstract

Measuring water current speed and direction of a long term underwater sensor (LoTUS) using tilt and roll compensation.

Marcus Lindkvist

Climate change brings upon melting of the Arctic ice and rising sea levels, which can be further understood by the collection of data underneath the Arctic ice caps. A Long Term Underwater Sensor (LoTUS) has therefore been proposed to be deployed under the ice caps for collection of water current speed and direction, along with temperature readings. In the current study a method to compute the water current speed and direction is experimentally verified using an accelerometer and magnetometer, where the results indicate that it can be used for scientific data collection.

Handledare: Jakob Kuttenkeuler
Ämnesgranskare: Uwe Zimmermann
Examinator: Tomas Nyberg
ISSN: 1401-5757, UPTEC F20 010

1 Populärvetenskaplig sammanfattning

Klimatförändrigarna gör att isarna vid nordpolen smälter i snabbare takt än någonsin tidigare. Hur snabbt och hur mycket som de kommer smälta i framtiden kan förutspås om man har tillgång till förlitlig data. Därför har en liten och tålig boj utvecklats med syfte att samla in information om hur havströmmarna under isarna beter sig och vilken temperatur det faktiskt är där. Kunskap om strömmarna hastighet och riktning kan hjälpa till att skapa mer noggranna klimatprognoser samt hur mycket havet kan komma att stiga inom en snar framtid. Genom att andvända matematiska samband har en uträkning av strömmens hastighet tagits fram och även testats. Det har visat sig att det går att uppskatta hastigheten och riktningen av vattenflöde med hjälp av metoden som presenteras i rapporten. För att göra det ännu bättre kan man behöva göra mer förarbete på själva sensorn genom att kalibrera den bättre eller använda en sensor som redan blivit mer noggrant kalibrerad.

Contents

2 Introduction

2.1 Background

Reliable data is necessary to understand natural processes, such as currents in the ocean, glaciers melting, rising sea levels and climate change. Sufficient and accurate readings of observed processes are also needed to create models that simulate the climate. It has been shown that the effects of climate change are creating a faster impact in the polar regions, which therefore is an important area to investigate more thoroughly [1]. Using a Long Term Underwater Sensor (LoTUS) could help to collect information about the water speed and direction under ice caps in the Arctic regions. Gathering data under the ice caps can help researchers to further understand the process of glaciers melting and thereby create more accurate global climate models, which can better predict raising sea levels [2].

The applications of the LoTUS are not restricted to data collection under ice caps, but can involve any type of bottom landing current measurement. These include, but are not limited to, ocean current speed and direction, stream velocity and tidal speed.

2.2 Properties of the Long Term Underwater Sensor (LoTUS)

LoTUS is a small (diameter of 254 mm), spherical buoy that weights 3 kg. It can withstand harsh environments and is durable for up to 10 years in order to collect data from arctic waters under a long period of time. Upon deployment, it sinks to the bottom and can withstand pressure up to 200 bars, allowing it to reach depth of approximately 2000 meters. Attachment of LoTUS consist of a 2m cylindrical rod and a mooring line that is connected to the anchor. For experiments in field within the report the a mooring line of length 0.5 is used due to shallow waters. When used in the ocean longer mooring line will be used to remove oscillations from vortex shedding. The length of the mooring line is, however, not within the scope of the project.

Collection of data will take place in intervals (and are saved on an internal memory) in order to save energy on the used batteries within. The collected data consists of the angle of tilt (θ) and the heading (ψ) of the spherically shaped buoy, as shown in figure 1, along with temperature readings.

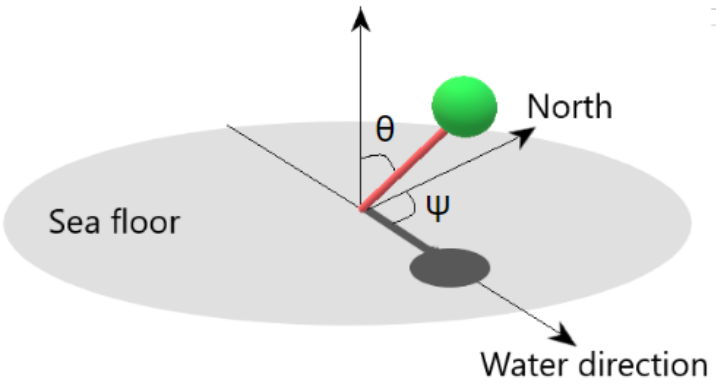

Figure 1: Illustration of LoTUS on the seafloor with an tilt angle (θ) and heading (ψ) caused by water flow.

Both tilt and heading are a result of water flow, where the water speed determines the tilt angle, demonstrated in figure 2, and its heading gives the direction at which the buoy will be leaning. The water direction can therefore be determining by the direction at which LoTUS is leaning.

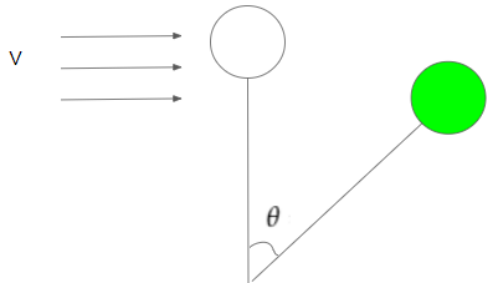

Figure 2: LoTUS tilts with an angle θ due to the incoming water flow at a speed v.

LoTUS is attached to an anchor by a stainless coil. When the collection of data is finished, a pre-set program activates a speed up of the erosion of the coil, which in turn, after 15 minutes, detaches LoTUS from the bottom. It will hence float up to the surface, where the buoy can easily be tracked by the implemented GPS system.

A previous study of Marchant et al (2014) suggests a method to determine water speed and direction using a tethered sphere, attached to the bottom with a rod and a tube. However, the tube restricts the sphere to rotate freely around its own axis (roll) when it has a constant heading. LoTUS will be able to rotate around its own axis and hence a tilt and roll compensation method

is suggested to take into account the effects of roll. Also, an uniform water flow is assumed in all future calculations along with LoTUS being stationary during sampling.

2.3 Scope of the report

The report covers the use of a low power, IMU-9250 sensor, to calculate water current speed and heading using a bottom landing, spherical tethered buoy (LoTUS).

2.4 Description of sensor

Inertial Measurement Units (IMU:s) are often used for determining the motion and orientation of an object by combining the use of an accelerometer, magnetometer and (for objects in motion) a gyroscope [4], which are all incorporated in the IMU-9250 sensor. For stationary objects the accelerometer and magnetometer are sufficient for determining its orientation along with its heading relative to the direction of Earth's magnetic field, since the compensation from the gyroscope is only used for moving objects.

Furthermore the IMU-9250 contains a temperature sensor and a precision clock that only drift with 1 % within the range of -40 to 85 °C. The VDD operating range is between 2.4V to 3.6V and the dimensions of the sensor is $3 \times 3 \times 1$ mm. Also, the sensor is resistant against shock up to 10,000g [4].

The sensor is powered by AA batteries within the scope of the report but different batteries will be used for long term deployment of LoTUS.

2.4.1 Accelerometer

Accelerometers can be used for measuring acceleration. It can be anything from the acceleration of a car to vibrations in the ground. However, if the accelerometer is stationary, it only measures the gravitational acceleration $\vec{a_g}$ acting upon it due to gravity [4], as shown in figure 3 . For an accelerometer with three axes, $\vec{a_g}$ can be displayed as a 3-dimensional vector in a Cartesian coordinate system. If the accelerometer is put on the ground, in a horizontal position, the z-axis of its internal reference frame will point straight up[3]. Also, the measured gravity vector will only point in the positive z-direction, since the force acting upon it comes from the ground and up, as shown in figure 3.

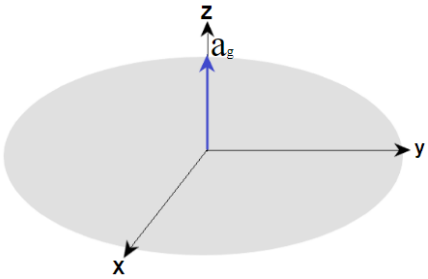

Figure 3: Gravitational acceleration $\vec{a_g}$ expressed as a vector in the accelerometer's coordinate system when put in a horizontal position.

There are different ways of determining acceleration within a sensor, where a change in capacitance is the used method within the MPU-9250[5]. Within the scope of the report, a capacitance accelerometer was used due to its general higher stability against temperature variation, along with a higher resolution [6].

The full scale range of the accelerometer is $\pm$1g $\pm$2g, $\pm$4g, $\pm$8g and $\pm$16g at a normal operating current of μA. Low power mode is also available for a current of 8.4 μA at 0.98Hz and 19.8μA at 31.25Hz. Furthermore, the MPU-9250's accelerometer have been industrially calibrated to limit thermal drift, with an accuracy of $\pm$ 0.026 %/°C [5].

2.4.2 Magnetometer

The magnetometer measures the direction and strength of Earth's magnetic field, using the Hall effect [5], which makes it useful for navigation. As for the acceleration vector, the measured magnetic field can be expressed in a 3-dimensional coordinate system.

Using the Hall effect to measure the magnetic field inside the magnetometer makes it temperature dependent [7]. However, unlike the accelerometer, the magnetometer has not been calibrated to be independent from changes in temperature. Using the magnetometer in temperatures other than 25 °C may be influenced by temperature-dependent readings [5].

The operating range of the magnetometer is $\pm$4800 μT for an operating current of 280µA at 8Hz, with a resolution of 14 bit (0.6µT/LSB).

3 Theory

3.1 Water speed calculation.

A water flow of speed v will cause LoTUS to tilt. However, the degree of tilt depends also on the buoyant and drag force of LoTUS, as shown in figure 4.

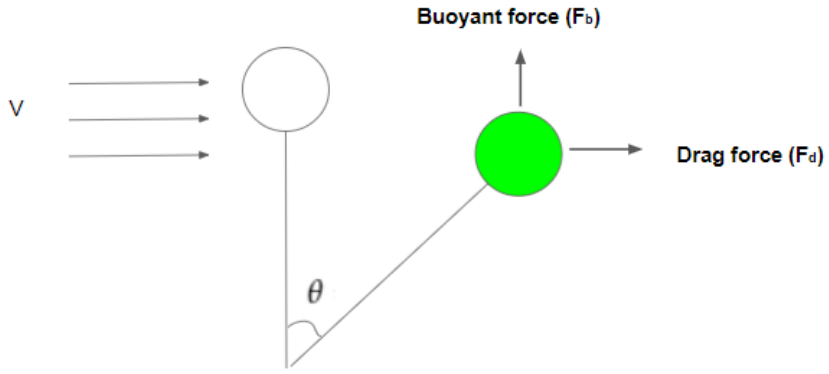

Figure 4:

The angle θ can therefore be determined as:

$$\theta = \arctan\left(\frac{F_d}{F_b}\right) \tag{1}$$

where F_d and F_b are given by:

$$F_d = \frac{1}{2}v^2\rho C_D A \tag{2}$$

$$F_b = (m - \rho V)g \tag{3}$$

where ρ, C_D, A, m, V, A and g are assumed constant and found in table 1. Solving for v by using equations 1-3 gives a simplified expression of water speed:

$$v = k\sqrt{\tan(\theta)} \tag{4}$$

where k is given by:

$$k = \sqrt{\frac{2(m - \rho V)g}{\rho C_D A}} \tag{5}$$

and m is the mass of LoTUS, ρ is water density, V is the volume of LoTUS, C_D is the drag force coefficient (which is approximated to 0.47 according to [**?**]) and V is the cross sectional area of LoTUS facing the current stream [16].

Table 1: Parameter values used in equation 5.

m	ρ	V	C_D	A	g
$3kg$	$997kg/m^3$	$0.00858m^3$	0.47	$0.0506m^2$	$9.82m/s^2$

3.2 Calculation of tilt and roll using an accelerometer.

Tilt (θ) and roll (ϕ) of a body can be determined using an accelerometer [8]. Gravitational acceleration is displayed as a 3-dimensional vector ($\vec{a_g}$) in the accelerometer's coordinate system, where θ is defined as the angle between the z-axis of the accelerometer and the measured $\vec{a_g}$, as displayed in figure 5.

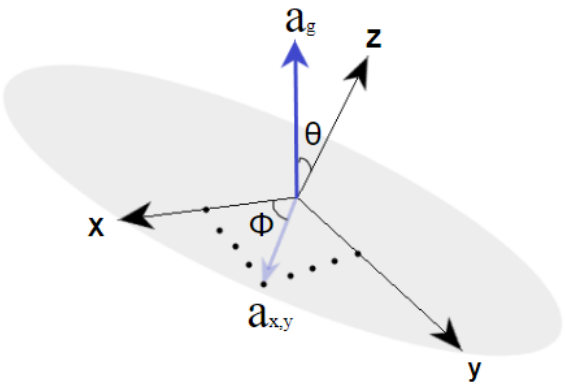

Figure 5: Coordinate system of the accelerometer after tilting with and angle θ and rolling with an angle ϕ. $\vec{a_g}$ is the gravity vector and $\vec{a_{x,y}}$ is the component of $\vec{a_g}$ in the x,y plane in the the accelerometer's coordinate system.

Furthermore, roll is defined to be the angle between the x-axis and the projected $\vec{a_g}$ onto the x,y plane ($\vec{a_{x,y}}$), which is simply the x and y values of $\vec{a_g}$. The two angles are calculated using the following equations:

$$\theta = \tan^{-1}\left(\frac{z^2}{\sqrt{x^2+y^2}}\right) \tag{6}$$

$$\phi = \tan^{-1}\left(\frac{y}{x}\right) \tag{7}$$

where x, y and z are the components of $\vec{a_g}$ in the accelerometer's coordinate system.

3.3 Tilt and roll compensation.

A coordinate system can be rotated around its own axes by using rotation matrices and thus changing the coordinates of a measured vector in the original

coordinate system [8]. Rotating a coordinate system (positioned with an initial tilt and roll) around its z-axis, with the same angle as it has rolled, will remove the roll, leaving a coordinate system that has only been tilted. Hence, it has been roll-compensated. Adding another rotation around the y-axis, with the angle of tilt, results in a coordinate system that has been both roll- and tilt-compensated. After roll and tilt compensation, in the case of an accelerometer, the measured $\vec{a_g}$ would point only in the z-direction.

Tilt and roll are calculated in equations 6 and 7 respectively and are used to construct two rotation matrices: $\cos\theta$

$$T_z = \begin{pmatrix} \cos(\phi) & -\sin(\phi) & 0 \\ \sin(\phi) & \cos(\phi) & 0 \\ 0 & 0 & 1 \end{pmatrix} \tag{8}$$

$$T_y = \begin{pmatrix} \cos(\theta) & 0 & \sin(\theta) \\ 0 & 1 & 0 \\ -\sin(\theta) & 0 & \cos(\theta) \end{pmatrix} \tag{9}$$

where T_z and T_y are the rotations around the z and y axis respectively. Applying T_z to a vector rotates the vector the same amount, and in the opposite direction, as it has rolled. Similarly, T_z rotates a vector as much as it has tilted, also in the opposite direction. Taking the inverse of equations 8, 9 will rotate the coordinate system instead of the vector. Multiplying the inverse of T_y and T_z together will perform two rotation on the coordinate system and, if applied to a vector, change the coordinate of the vector.

$$T = T_y^{-1}T_z^{-1} = \begin{pmatrix} \cos(\theta) & 0 & \sin(\theta) \\ 0 & 1 & 0 \\ -\sin(\theta) & 0 & \cos(\theta) \end{pmatrix}^{-1} \begin{pmatrix} \cos(\phi) & -\sin(\phi) & 0 \\ \sin(\phi) & \cos(\phi) & 0 \\ 0 & 0 & 1 \end{pmatrix}^{-1} \tag{10}$$

Applying the rotation matrix in equation 10 to any measurement of the sensor, will result in a vector as if measured in a coordinate system that is located horizontally. Any data can therefore be transformed to be measured in a sensor that has neither been tilted, nor rolled. If equation is applied to the the readings of the accelerometer, it will therefore measure gravity only in the z-direction:

$$T\vec{a_g} = [0, 0, 1] \tag{11}$$

The rotations made by equation 10 are demonstrated in figure 6, using an arbitrary vector from the accelerometer. First, there is a rotation of the coordinate system around the z-axis with an angle α, to compensate for roll. Secondly, the tilt compensation takes place by a rotation around the y-axis with an angle β, which results in a coordinate system that measures $\vec{a_g}$ only in the z-direction.

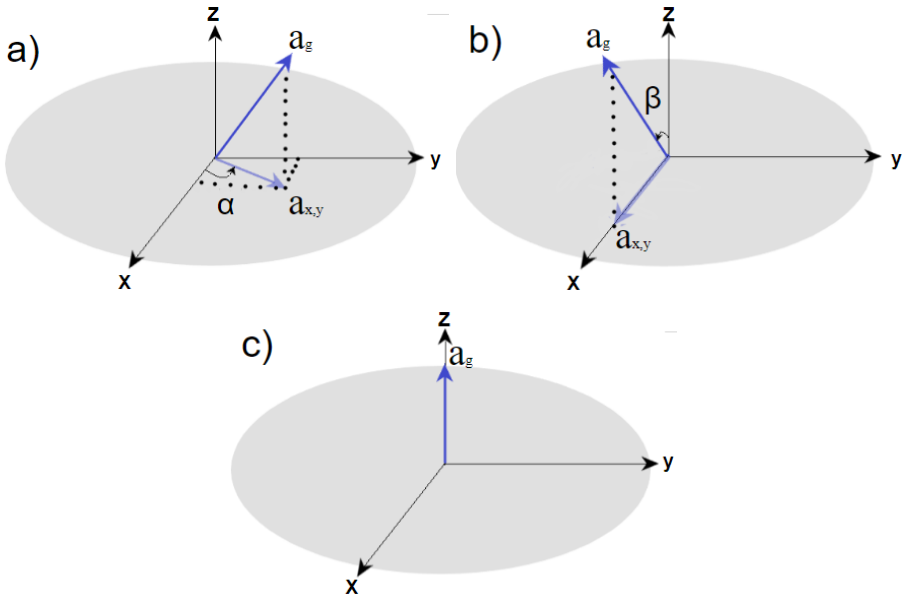

Figure 6: The gravity vector $\vec{a_g}$, measured in the sensor when in an arbitrary position a). The coordinate system in b) is showing $\vec{a_g}$ after a rotation around the z-axis by the angle α. Another rotation around the y-axis with an angle β gives the vector in c). $\vec{a_x, y}$ is the projection of $\vec{a_g}$ onto the x,y-plane in the accelerometer.

3.4 Linear temperature dependency

Both the accelerometer and magnetometer could be temperature-dependent and, in some cases, linearly [9], [10], [11]. Therefore, offsets due to temperature change can be compensated for, if the change in measured data relative to temperature is known.

One method of determining a linear slope from a data set is the method of linear least squares. Given a measured value y_i at x_i, a linear approximation of the measurement can be expressed by:

$$y_i = b_0 + b_1 x_i \tag{12}$$

where b_0 is the y intersect and b_1 is the slope of the linear approximation. According to the least square method, b_0 and b_1 are found by computing the minimum residuals from equation 12 in the following way:

$$S(b_0, b_1) = \sum_{i=1}^{n} (y_i - b_0 + b_1 x_i)^2 \tag{13}$$

$$\frac{\partial S(b_0, b_1)}{\partial b_0} = 0 \tag{14}$$

$$\frac{\partial S(b_0, b_1)}{\partial b_1} = 0 \tag{15}$$

Solving equations 14 and 15 as a linear set of equations will give the values of b_o and b_1 and, if they are put into equation 12, gives the best linear fit of the data.

The slope the linear fit, b_1, can be used to compensate for temperature dependency of the measurement:

$$\psi = b_1(T - T_{ref}) + \psi_{measured} \tag{16}$$

$$\theta = b_1(T - T_{ref}) + \theta_{measured} \tag{17}$$

where T is the current temperature measured by the sensor and T_{ref} is a reference temperature.

3.5 Calibration of the magnetometer

The magnetic field measured by a magnetometer is subject to disturbances, such as from hard and soft magnetic materials, along with the scaling and bias errors from manufacturing. The mentions disturbances will result in a shift and scaling of the data measured by the magnetometer. One approach to compensate for such effects is the method of ellipsoid fitting [12].

Rotating a magnetometer in a spherical pattern will give values in the xy, xz and yz plane in the magnetometer, matching an elliptical shape if the magnetometer is subject to the mentioned disturbances. Furthermore, the ellipse will also be shifted from its center, as seen in figure 7.

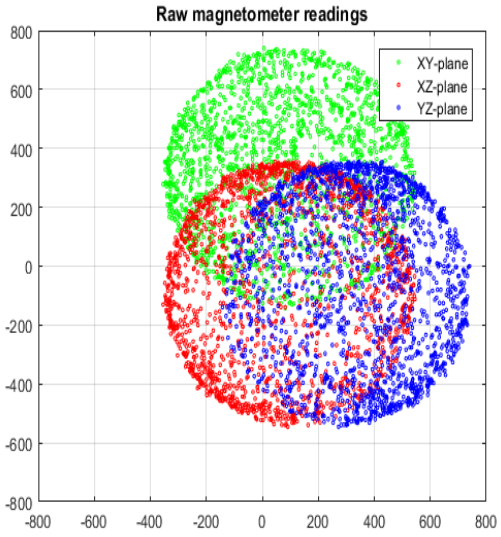

Figure 7: Raw data from measuring the magnetic field using a magnetometer.

The method of ellipsoid fitting will shift the ellipse back to its center and scale it into a sphere, thereby removing effects from hard and soft magnetic materials along with scaling errors from manufacturing [12]. Using ellipsoid fitting on the ellipses in figure 7 can be seen in figure 8

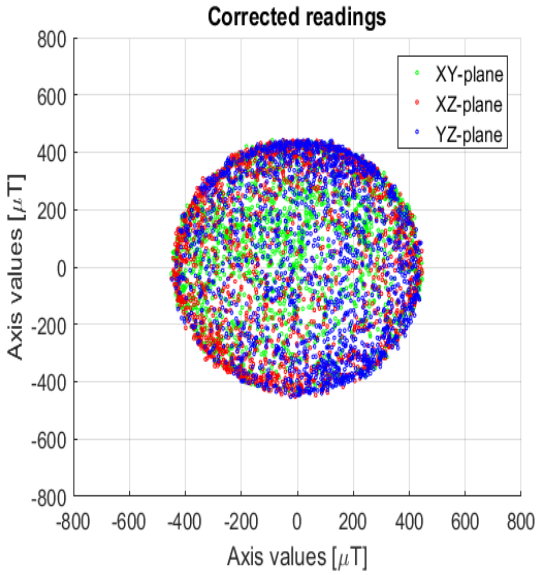

Figure 8: Corrected data using the method of ellipsoid fitting.

4 Method

4.1 Ellipsoid fitting of magnetometer

Scaling errors, soft and hard iron effect were accounted for by using ellipsoid fitting. The sensor was rotated freely in space, collecting data of the magnetic field. After the collection of data ellipsoid fitting was made to shift and scale the measured magnetic field to remove disturbances.

A bias ($\vec{m}_{bias}$) and scaling vector ($\vec{m}_{scale}$) was given by the ellipsoid fitting, where $\vec{m}_{bias}$ first was added to the data from the magnetometer to remove offset errors. After the addition, $\vec{m}_{scale}$ was multiplied with the new, non-bias vector, to remove scaling errors.

$$\vec{m} = \vec{m}_{scale}(\vec{m}_{raw} + \vec{m}_{bias}) \tag{18}$$

where $\vec{m}_{raw}$ is the raw magnetometer data and $\vec{m}$ is the calibrated magnetic vector.

4.2 Initial calibration of sensor coordinate system.

The sensor was originally mounted on a plate in a horizontal position, to represent LoTUS standing upright in waters without any oceanic current. All collected data was first normalized, meaning that instead of the accelerometer

reading $a_g = [a_x, a_y, a_z]g$ it measured $a_g = [a_x, a_y, a_z]$ with a maximum value on any axis equal to 1.

An initial measurement from the accelerometer ($\vec{a_0}$) was taken. It was noted that the x,y-plane of the sensor initially was not in line with the horizontal set up, since the measurement did not read $\vec{a_0}$= [0,0,1]. Therefore, initial tilt (θ_0) and roll (ϕ_0) was measured from $\vec{a_0}$, by using equations 6 and 7, even though no tilt nor roll had been applied to the sensor.

A calibration matrix, T_0, was constructed as described by equation 10, where the initial angles θ_0 and ϕ_0 of $\vec{a_0}$ were used.

$$T_0 = \begin{pmatrix} \cos(\theta_0) & 0 & \sin(\theta_0) \\ 0 & 1 & 0 \\ -\sin(\theta_0) & 0 & \cos(\theta_0) \end{pmatrix}^{-1} \begin{pmatrix} \cos(\phi_0) & -\sin(\phi_0) & 0 \\ \sin(\phi_0) & \cos(\phi_0) & 0 \\ 0 & 0 & 1 \end{pmatrix}^{-1} \tag{19}$$

T_0 was multiplied with $\vec{a_0}$ in order to calibrate the coordinate system of the accelerometer, so that it would measure as if the accelerometer was standing in a horizontal position:

$$\vec{a_0}' = T_0\vec{a_0} = [0, 0, 1] \tag{20}$$

where $\vec{a_0}'$ is the gravitational acceleration measured in the calibrated accelerometer. Doing so gave readings as if the sensor was perfectly installed in LoTUS. Also, the horizontal position of the sensor represented a position of LoTUS where no water current was present. Therefore, the z-axis of the sensor and LoTUS were aligned via the calibration process.

A reference vector of the magnetic field ($\vec{m_0}$) was also collected. The calibration matrix, T_0, in equation 19 was multiplied with $\vec{m_0}$ to rotate the coordinate system of the magnetometer into the same as the accelerometer.

$$\vec{m_0}' = T_0\vec{m_0} \tag{21}$$

where $\vec{m_0}'$ is the field of Earth's magnetic north, measured in the calibrated coordinate system of the magnetometer.

The initial yaw ($\vec{\psi_0}$) was defined as how much $\vec{m_0'}$ had rolled. Therefore, the initial yaw angle was given by:

$$\psi_0 = \tan^{-1}\left(\frac{m_{0y}'}{m_{0x}'}\right) \tag{22}$$

where m_{0x}' andm_{0y}' are the x and y components of $\vec{m_0'}$ respectively.

4.3 Calculating tilt, roll and yaw.

The position of the sensor was altered with known inclinations of 0-30 degrees of tilt with 10 degrees between steps. Furthermore, it was positioned at known

yaw angles ranging from 0-180 degrees of yaw with 60 degree intervals.

For each position of the sensor the calibration matrix ($T_{o,}$) in equation 19 was applied to the data from the accelerometer ($\vec{a}$) and magnetometer ($\vec{m}$) in order to mathematically align the z-axis of the sensor with the z-axis of LoTUS.

$$\vec{a}^{'} = T_0 \vec{a} \tag{23}$$

$$\vec{m}^{'} = T_0 \vec{m} \tag{24}$$

Therefore, all data represents the LoTUS coordinate system instead of the sensor's coordinate system.

Tilt and roll was computed for each position of the sensor by using equations 6 and 7 on the vector $\vec{a}^{'}$. The two angles were used to compute a tilt and roll compensation matrix as described in equation 10:

$$T = \begin{pmatrix} \cos(\theta) & 0 & \sin(\theta) \\ 0 & 1 & 0 \\ -\sin(\theta) & 0 & \cos(\theta) \end{pmatrix}^{-1} \begin{pmatrix} \cos(\phi) & -\sin(\phi) & 0 \\ \sin(\phi) & \cos(\phi) & 0 \\ 0 & 0 & 1 \end{pmatrix}^{-1} \tag{25}$$

The first step of calculating yaw was to apply T to the calibrated data from the magnetometer ($\vec{m}^{'}$), to remove tilt and roll of the sensor.

$$\vec{m}^{''} = T\vec{m}^{'} \tag{26}$$

where $\vec{m}^{''}$ is the magnetic north measured in a coordinate system as if LoTUS was standing in an upright position, without any roll of tilt.

Yaw was the only remaining angle, since it was not removed in the tilt and roll compensation, and could therefore be calculated in the same way as roll:

$$\psi^{'} = \tan^{-1}\left(\frac{m_y^{''}}{m_x^{''}}\right) \tag{27}$$

where $\psi^{'}$ is the yaw angle in the calibrated coordinate system that has been tilt and roll compensated, $m_x^{''}$ and $m_y^{''}$ are the x and y components of $\vec{m}^{''}$ respectively. To get the true yaw angle the following equation was used:

$$\psi = \psi^{'} - \psi_0 \tag{28}$$

4.4 Field testing

The initial calibration was made by putting LoTUS in still water to collect a reference vector, ($\vec{a_0}$), in the same way as for the lab testing on the horizontal

plate. All steps of calculation as mentioned in section 4.2 was made using $\vec{a_0}$.

After the initial calibration, LoTUS was put into a water flow with a depth of 3 meters during a period of 2 hours. One measurement was taken every 20 second in order to prevent heating of the sensor, which may affect the results, and to save energy consumption of the batteries. For each measurement of the sensor the same calculation, as in the lab testing, to calculate tilt and yaw was carried out. The data was post processed by the implementation of the filter seen in equation 29 in order to remove noise in the data.

The water flow speed was roughly estimated to be 0.3 m/s, after 30 minutes of measuring, by taking 5 samples of moving object on the water and timing how long it took to travel 2 meters.

4.5 Determining sensor temperature dependency in lab

Two experiments were made to test the temperature dependency of the sensor. In the first experiment the sensor was put into a refrigerator for 46 hours at a known tilt of 10°tilt and a constant yaw angle. In the third experiment the sensor was put in a sheltered location, outdoors, in order to get slow and natural changes in temperature. Furthermore, the sensor was stationary during both experiments in order to note any changes due to temperature change.

Equations 16 and 17 where used to compute a linear approximation of the temperature dependency for each experiment. Also, a moving average filter was used to reduce noise in the a measurement, creating filtered value y(n):

$$y(n) = \frac{1}{length}(x(n) + x(n-1) + ... + x(n-(length-1))) \tag{29}$$

where x(n) is the nth measurement of x and *length* are the number of values used to create one filtered value. Length was set to 5.

5 Results and discussion

5.1 Calibration of the sensor's coordinate system.

The accelerometer used inside the LoTUS should measure gravitational acceleration only in the downward direction when LoTUS is orthogonal to the horizontal plane (standing in a upright position due to no oceanic currents). However, the sensor will not be perfectly installed, meaning that the accelerometer reads a vector $\vec{a_0} = [a_x.a_y, a_z]$ instead of $\vec{a_0} = [0, 0, 1]$ (after normalization of the vector), when LoTUS is in an upright position. Therefore, an initial calibration of the sensor's coordinate system is necessary.

Adjusting the z-axis of the accelerometer with the z-axis of LoTUS can be

done by rotation the coordinate system of the sensor such that the measured gravity vector is $\vec{a_g}$=[0,0,1] inside the sensor, using the tilt and roll compensation method as done in section 4.2. Since LoTUS is standing upright when measuring $\vec{a_0}$, its z-axis is pointing straight down, which is the same direction as the known gravity vector $\vec{a_g}$. Therefore, adjusting the z-axis of the sensor with $\vec{a_g}$ will calibrate the coordinate system of the sensor such that the z-axis of the sensor is pointing in the same direction as the z-axis of LoTUS.

All measurements taken from the magnetometer are rotated with the same calibration matrix as the accelerometer, in order for the accelerometer and magnetometer to be in the same coordinate system. Applying T_0 to all measurements of the sensor will calibrate the coordinate system such that it is relative the LoTUS body instead of the sensor, which is what is wanted. Without T_0, a rotation around the z-axis of LoTUS would be represented as an arbitrary rotation of the coordinate system of the sensor. The sensor is therefore experiencing a rotation around an arbitrary axis and will measure different tilt and yaw angles when LoTUS is rolling, giving non-reliable measurements for determining current speed and direction. This is true even if LoTUS is rolling at a fixed yaw angle.

5.2 Calculation of tilt and yaw in lab

Measured tilt and yaw are shown in figure 9 and 10 respectively, where four known position of the sensor are displayed for each angle. The measured tilt angles match the known inclination with an standard deviation of ± 0.0294 degrees, while the standard deviation is 2.5 degrees for the yaw angle. The spread is 0.1689 degrees for measured tilt and 12.9 degrees for measured yaw.

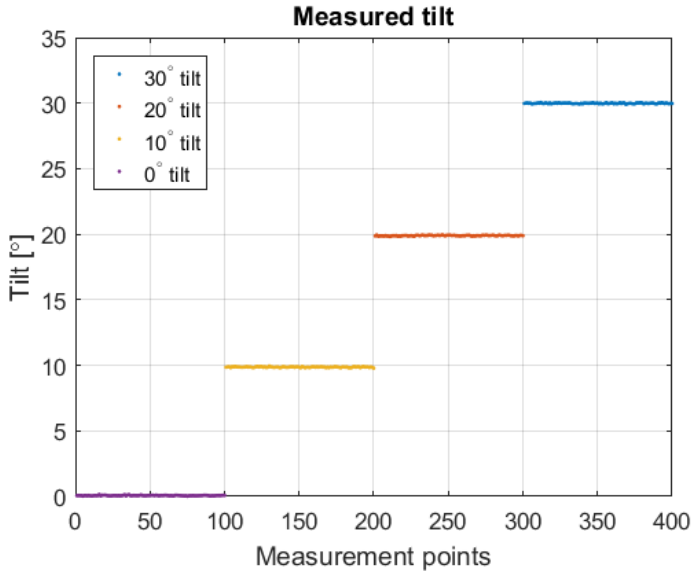

Figure 9: Measured tilt at known inclinations of 0, 10, 20 and 30 degrees.

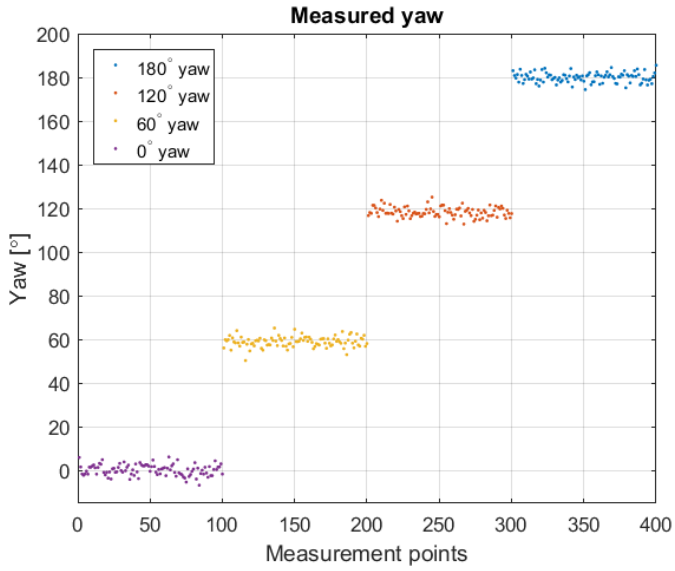

Figure 10: Measured yaw at known heading of 0, 60, 120 and 180 degrees.

There is a larger variation in yaw compared to tilt, which is assumed to originate from the variation of measured magnetic field. Natural variations in the

earth magnetic field along with local changes due to electricity and metallic object influences the measured magnetic field and hence the measured yaw [13]. However, the spread is maximum $\pm$ 12.9 degrees in yaw and can therefore be used to approximate the direction of water flow. One way of reducing the spread is by implementing the filter in equation 29, at the cost of precision.

5.3 Temperature dependency

The temperature dependency is expected to be linear with temperature, which is observed in figures 11 and 12. However, the slope of temperature dependency in figure 12, for the yaw angle, differs between experiment 1 and 2. The yaw angle from experiment 2 did not show the same amount of change due to temperature as in experiment 1, which most likely is due to the calibration temperature. In experiment 1 the sensor was calibrated at 24 °C before if was put into the refrigerator, while it was calibrated at 15 °C for experiment 2. A larger gap between calibration temperature and observed temperature will give larger errors due to the temperature dependency. The bigger spread in experiment 1 compared to experiment 2 is therefore to be expected.

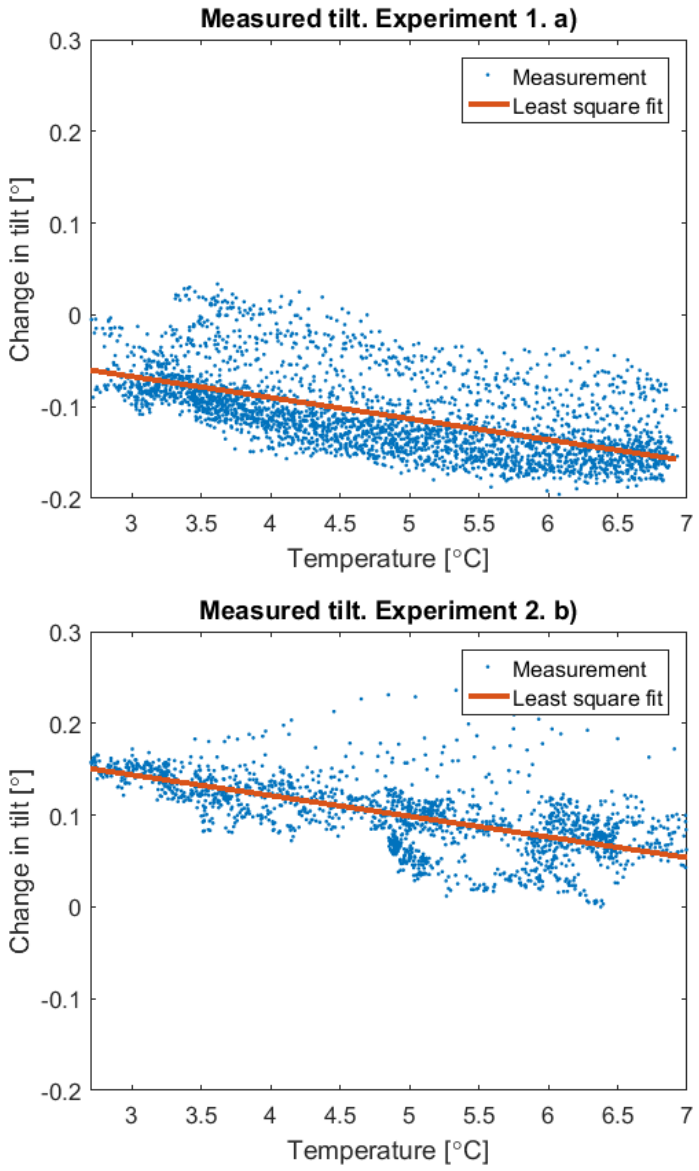

Figure 11: Measured tilt at constant inclination in experiment 1 a) and experiment 2 b)

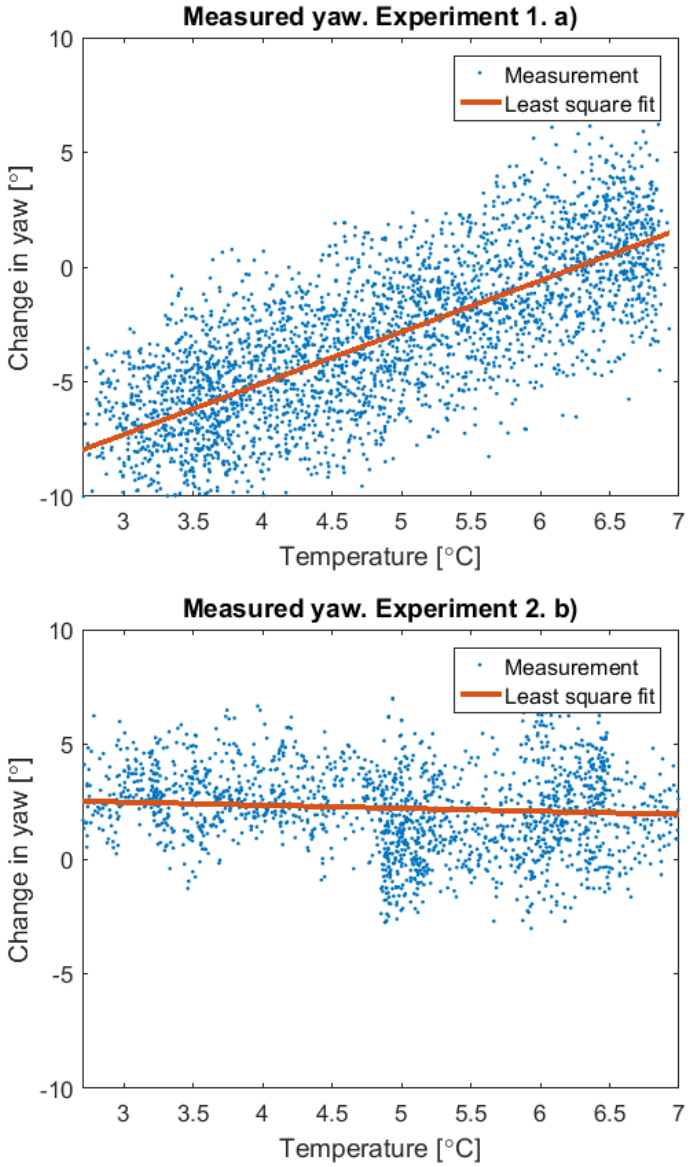

Figure 12: Measured yaw at constant heading for experiment 1 a) and experiment 2 b)

In figure 11, the slope at which the angle of tilt varies with temperature, has been estimated to be -0.0225 degrees per Celsius for experiment 1 and -0.0230 for experiment 2, using least squared fitting to the data. Similarly, in figure 12. the slope at which the angle of yaw varies with temperature, has been estimated to be 2.235 degrees per Celsius for experiment 1 and -0.1330 for ex-

periment 2.

The slope of temperature dependency for the accelerometer was almost identical, and relatively small, in experiment 1 and 2. The reason for this could be the fact that it was temperature calibrated before use, unlike the magnetometer.

Furthermore, calibration temperature may not be the only cause of fluctuations in the results, since the temperature dependency may change with position [9]. Also, the temperature dependency may change depending on whether the temperature is increasing or decreasing. This was not tested within the scope of the report but could help explain the reason why the temperature dependency differs between the two experiments. As seen in figure 13, the two different temperature profiles for each experiment is not identical. Since the results may be dependent on how fast and, whether or not the temperature is increasing or decreasing, the two different temperature profiles could help explain the difference in results between experiment 1 and 2.

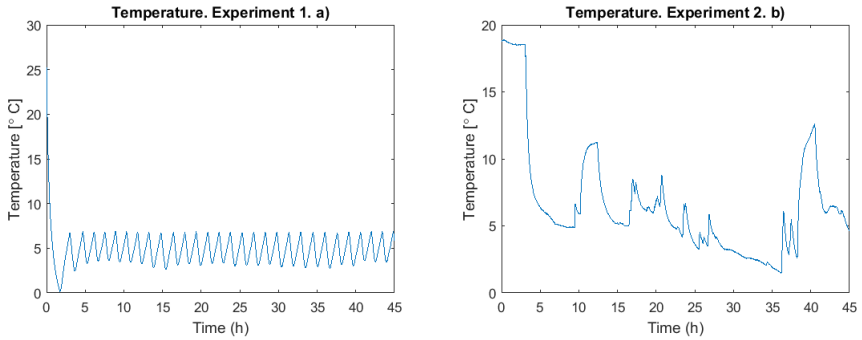

Figure 13: Temperature profiles for experiment 1 a) and experiment 2 b).

Another cause of disturbance in experiment 1 is the refrigerator itself. As it turns on the electric field inside is altered, which has a direct effect on the magnetometer and hence the measured yaw.

Temperature compensation can only be made at a specific position the sensor, due to its linearity, but as the temperature dependency changes with orientation a linear compensation could not be used. A more thorough investigation of temperature dependency needs to be made, where the sensor is exposed for different temperatures while altering its position [9]. A polynomial expression can therefore be found that could remove 95% of the temperature dependency.

Furthermore, a change in temperature of 4 °C showed a maximum $\pm$ 8 de-

gree yaw difference in experiment 1, as seen in figure 12. In the Arctic region, where LoTUS may be deployed, water temperature vary with up to 2 °C on annual average [14]. A 2 °C change which would result in a $\pm$ 4 degree change in yaw due to temperature.

5.4 Calculation of tilt and yaw in field

During the sampling in field it was noted that the LoTUS buoy was not standing still. Yaw oscillations, caused by vortex shedding, along with rolling and variations in water speed all contribute to alter the readings inside the accelerometer due to acceleration. As the tilt angle is being altered due to changes in direction during a measurement, so will the measured yaw angle. Therefore, the results in tilt and yaw, in figure 14 and 15 respectively, are expected to contain errors causes by acceleration, since all calculations are based on a stationary LoTUS. Also, vortex shedding will give oscillating water directions measured be LoTUS, which can be seen in figure 15. Even though the water direction is constant, the measured heading of LoTUS changes from 30 to 70 degrees during short time intervals.

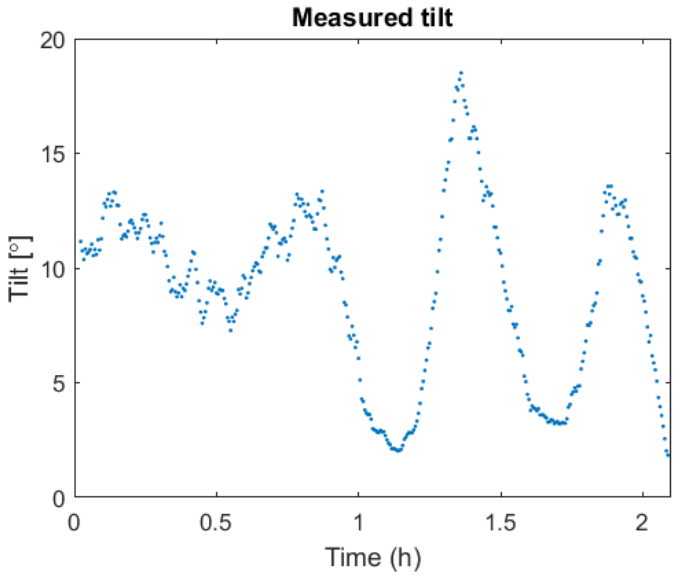

Figure 14: Measured tilt in stream.

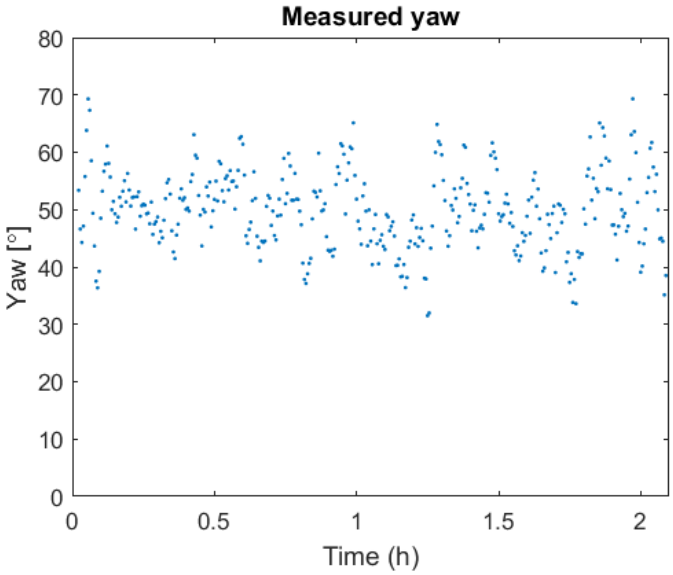

Figure 15: Measured yaw in stream with heading estimated to be 40 °north

.

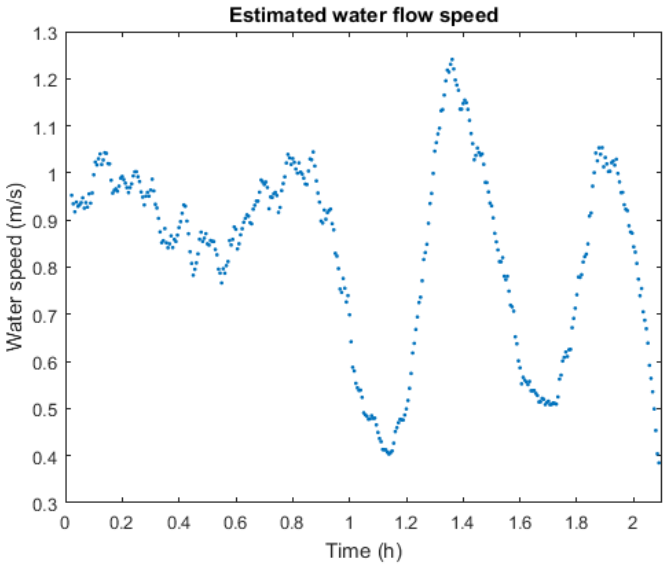

Figure 16: Measured water flow speed using equation 4 along with the tilt angles from figure 14.

It was concluded, in section 5.3, that the sensitivity to temperature variations

increases the larger the difference is between measured temperature and calibration temperature. Therefore, due to the temperature variation measurement in the field, variation in measured tilt and yaw is expected if the temperature moves away from the calibration temperature, which was at 7.4 °C. Since the temperature during the field testing was close to the calibration temperature, no major visible effects from temperature can be seen. However, in figure 14, the measured tilt angle contains more noise in the first hour compared to the second. One explanation could be due to the higher temperature during the first hour since the sensor had not reached the temperature of the surrounding water. The temperature profile for the field testing can be seen in figure 17, where the temperature inside the LoTUS buoy decreases during data collection.

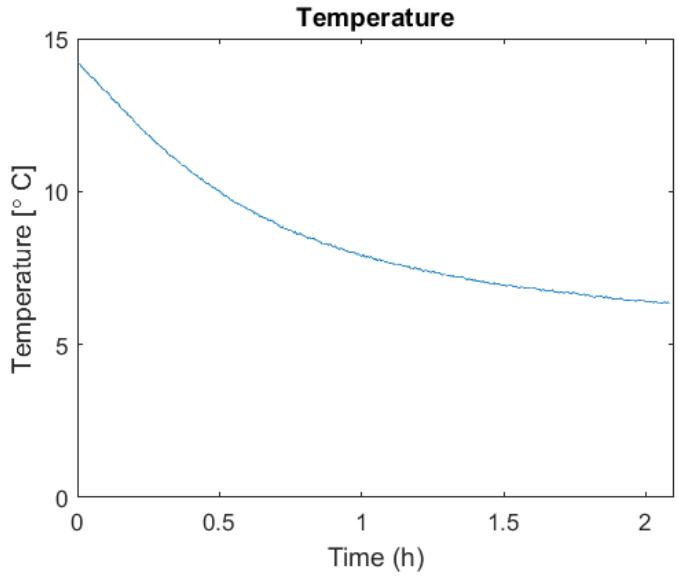

Figure 17: Temperature profile during 2 hours in the stream.

As mentioned in section 4.4, an approximation of the water flow speed was estimated to 0.3 m/s after 30 minutes of LoTUS being in the water. Looking at figure 16, after 0,5 hours, shows values between 0.78-0.9 m/s. The measured speed are approximately 2.5-3 times larger than observed, which can have several explanations.The most likely explanation is from the movement of the buoy, since the calculation is based on a stationary sensor. As mentioned earlier, LoTUS was moving due to change in water speed along with vortex oscillations, both contributing to acceleration of the accelerometer.

Another reason could be that the shape of LoTUS contains flaws such the approximation of the water speed in not complete. Errors from the water estimation could therefore contribute to the difference between observation and measured data.

Furthermore, the approximation of the observed water speed could be wrong. Since it was made by measuring the speed of leaves on the surface of the water flow it can be effected by wind, that may reduce the speed of the leaves. However, a more controlled environment of known water speeds needs to be made in order to draw any accurate conclusions from the water speed approximation from LoTUS when it was tested in the field.

6 Improvements

A magnetometer that has been temperature calibrated will remove temperature dependency of measured yaw angle. Since the arctic water temperature is not constant, using the existing magnetometer will cause errors due to temperature drift.

A Kalman filter, instead of a moving average filter, could be used to reduce the noise of the data from the magnetometer [17].

Vortex shedding was noted during the experiments and is causing unwanted movement of the LoTUS buoy. To remove such effect the design of the hydrodynamic shape needs to be looked over. Also, the length of the anchor line could be increased. Furthermore, another way to remove errors caused by movement during measurement is to implement of a gyroscope [15].

A local calibration method would increase the accuracy of the measurement since the ellipsoid fitting needs to be made where the LoTUS will take its measurement. The magnetic field where LoTUS takes its measurement needs to be identical where the calibration takes place. Otherwise the ellipsoid fitting will not remove the magnetic disturbances.

7 Conclusion

The proposed tilt and roll method can be used to calculate current speed and direction of the LoTUS buoy, using an accelerometer and a magnetometer. Also, the calculation was more accurate when the sensor was stationary, since movements of the sensor during measurement will give different vectors of acceleration then only measuring the gravitational acceleration. Therefore, the design of LoTUS should be investigated to make it more flow dynamic in order to remove motion when in a water flow.

Variation in the results will depend on the temperature dependency of the magnetometer, which needs to be removed in order to collect reliable results over a long period of time. The magnetometer will give different result when the temperature changes, even if the position is kept constant. A thorough temperature dependency investigation need to be made to remove such ef-

fects, or change the magnetometer to one that has already been temperature calibrated.

References

[1] JOHANNESSEN, O.M., BENGTSSON, L., MILES, M.W., KUZMINA, S.I., SEMENOV, V.A., ALEKSEEV, G.V., NAGURNYI, A.P., ZAKHAROV, V.F., BOBYLEV, L.P., PETTERSSON, L.H., HASSELMANN, K. CATTLE, H.P. 2004, Arctic climate change: observed and modeled temperature and sea-ice variability, Munksgaard International Publishers, 9600 Garsington Road , Oxford OX4 2DQ , UK , USA.

[2] chlegel, N., Seroussi, H., Schodlok, M.P., Larour, E.Y., Boening, C., Limonadi, D., Watkins, M.M., Morlighem, M., van den Broeke, Michiel R. info:eu-repo/dai/nl/073765643 2018, Exploration of Antarctic Ice Sheet 100-year contribution to sea level rise and associated model uncertainties using the ISSM framework, Copernicus GmbH.

[3] Talat Ozyagcilar. Implementing Tilt-Compensate eCompass using Accelerometer and Magnetometer Sensors. 2015 Nov. Document Number: AN4248

[4] S.V. Ghasemzade and F. Jamshidi. Applications of Inertial Navigation Systems in Medical Engineering. J Biomed Phys Eng. 2018 Sep; 8(3): 325–332.

[5] InvenSense Inc. MPU-9250 Product Specification Revision 1.1. 2016 jun 06. Document Number: PS-MPU-9250A-01

[6] N.C. Yoder, D.E. Adams, in Sensor Technologies for Civil Infrastructures. Commonly used sensors for civil infrastructures and their associated algorithms. 2014.

[7] Shiraguppe, R., Shiraguppe, K., Shiraguppe, V. TEMPERATURE DEPENDENCE OF HALL EFFECT. International journal och advance research in science and engineering. Vol. 07, no. 01. March 2018

[8] Mark Pedley. Freescale Semiconductor, Inc. Tilt Sensing Using a Three-Axis Accelerometer. 2013 March 06. Document Number: AN3461

[9] Ruzza, G., Guerriero, L., Revellino, P. Guadagno, F.M. 2018, "Thermal Compensation of Low-Cost MEMS Accelerometers for Tilt Measurements", Sensors (Basel, Switzerland), vol. 18, no. 8, pp. 2536

[10] Cholakova, I.N., Takov, T.B., Tsankov, R.T. Simonne, N. 2012, "Temperature influence on Hall effect sensors characteristics", IEEE, , pp. 967.

[11] He, J., Zhou, W., Yu, H., He, X. Peng, P. 2018, "Structural Designing of a MEMS Capacitive Accelerometer for Low Temperature Coefficient and High Linearity", Sensors (Basel, Switzerland), vol. 18, no. 2, pp. 643.

[12] Liu, D., Pei, L., Qian, J., Wang, L., Liu, C., Liu, P. Yu, W. 2016, "Simplified ellipsoid fitting-based magnetometer calibration for pedestrian dead reckoning", , pp. 473.

[13] Wu, J. 2019, "Real-Time Magnetometer Disturbance Estimation via Online Nonlinear Programming", IEEE Sensors Journal, vol. 19, no. 12, pp. 4405-4411

[14] Ned Allen Ostenso. Encyclopædia Britannica, inc. Arctic Ocean. December 19, 2018. Available from: https://www.britannica.com/place/Arctic-Ocean/Topography-of-the-ocean-floorref910443 [09 Feb 2020]

[15] El-Diasty, M. 2014, "An Accurate Heading Solution using MEMS-based Gyroscope and Magnetometer Integrated System (Preliminary Results)", ISPRS Annals of Photogrammetry, Remote Sensing and Spatial Information Sciences, vol. II-2, no. 2, pp. 75-78.

[16] Marchant, R., Stevens, T., Choukroun, S., Coombes, G., Santarossa, M., Whinney, J. Ridd, P. 2014, "A Buoyant Tethered Sphere for Marine Current Estimation", IEEE Journal of Oceanic Engineering, vol. 39, no. 1, pp. 2-9.

[17] Beravs, T., Begus, S., Podobnik, J. Munih, M. 2014, "Magnetometer Calibration Using Kalman Filter Covariance Matrix for Online Estimation of Magnetic Field Orientation", IEEE Transactions on Instrumentation and Measurement, vol. 63, no. 8, pp. 2013-2020.